3746 *Chem. Mater.* **2010,** *22,* 3746–3751
DOI:10.1021/cm100673s

CHEMISTRY OF MATERIALS
Article

In situ SAXD Studies on Phenylene- and Thiophene-Bridged Periodic Mesoporous Organosilicas (PMOs)

Vivian Rebbin,*[,†] André Rothkirch,[†] Michael Fröba,[‡] and Sérgio S. Funari[†]

[†]*HASYLAB@DESY, Notkestrasse 85, 22607 Hamburg, Germany, and* [‡]*Institute for Inorganic and Applied Chemistry, University of Hamburg, Martin-Luther-King-Platz 6, 20146 Hamburg, Germany*

Received March 5, 2010. Revised Manuscript Received April 23, 2010

In situ small-angle X-ray diffraction (SAXD) investigations are carried out in order to obtain an insight into the formation process of 2D hexagonal ordered phenylene- and thiophene-bridged periodic mesoporous organosilicas (PMOs) synthesized with Brij 76 (polyethylene (10) stearylether). The reaction solution is investigated by pumping it through a capillary placed in a synchrotron radiation beam. Data collection is stopped when the growing particle size lead to an irregular flow of the solution. The resulting data is compared with powder X-ray diffraction of the samples synthesized in the laboratory. The 2D hexagonal ordered PMO products synthesized with Brij 76 are formed via a metastable three-dimensional hexagonal ordered transition state. Here, we describe the formation process of the PMO materials regarding the properties of the structure-directing agent.

1. Introduction

Since 1992, when the Mobil Oil group first discovered the ordered mesoporous silica materials,[1,2] a lot of interest has been put on their self-assembling process during the formation of the structure. The mesophase, as well as the formation process, can be influenced by parameters such as temperature, pH, and mainly the concentrations of the structure-directing agent and the silica precursor.

The formation mechanism can partly be explained by the concept of the ion pair packing parameter g originally designed for the description of surfactant organization in amphiphilic liquid crystalline arrays: $g = V/(a_0 l)$, where V is the total volume of the surfactant chains plus any cosolvent organic molecules between the chains, a_0 is the effective headgroup area at the micelle surface, and l is the kinetic surfactant tail length or the curvature elastic energy.[3] High g values stabilize low curved surfaces such as the lamellar structure (space group $p2$, $g \approx 1$). Lower g values lead to higher curved surfaces like the bicontinuous cubic structure (space group $Ia3d$ with $g \approx 2/3$) or the 2D hexagonal ordered structure (space group $p6mm$ with $g \approx 1/2$). Packing parameters below 1/2 stabilize structures formed by different organization of micelles, like cubic structures (space groups $Pm3m$, $Fm3m$, $Im3m$) or the 3D hexagonal ordered structure with the space group $P6_3/mmc$. During the formation process, the most important factors are the multidentate binding of silicate oligomers, preferred polymerization of silica at the silica/surfactant interface, and charge density matching.[4]

Various in situ small-angle X-ray diffraction (SAXD) studies deal with the formation processes of different mesoporous silica materials, e.g., the MCM-41 and the SBA-15 silica are well-established.[5−16] Different mechanisms induced by different pH values are used to explain the syntheses. In the case of the MCM-41, trialkylammonium halides in basic solution utilized as structure-directing agents and the cationic headgroups of the surfactant interact directly with the anionic silica species during the formation. In contrast, SBA silica materials, for example,

*Vivian.Rebbin@desy.de.

(1) Kresge, C. T.; Leonowicz, M. E.; Roth, W. J.; Vartuli, J. C.; Beck, J. S. *Nature* **1992**, *359*, 710.
(2) Beck, J. S.; Vartuli, J. C.; Roth, W. J.; Leonowicz, M. E.; Kresge, C. T.; Schmitt, K. D.; Chu, C. T-W.; Olson, D. H.; Sheppard, E. W.; McCullen, S. B.; Higgins, J. B.; Schlenker, J. L. *J. Am. Chem. Soc.* **1992**, *114*, 10834.
(3) Huo, Q.; Margolese, D. I.; Stucky, G. D. *Chem. Mater.* **1996**, *8*, 1147.
(4) Monnier, A.; Schüth, F.; Huo, Q.; Kumar, D.; Margolese, D.; Maxwell, R. S.; Stucky, G. D.; Krishnamurty, M.; Petroff, P.; Firouzi, A.; Janicke, M.; Chmelka, B. F. *Science* **1993**, *261*, 1299.
(5) Gross, A. F.; Ruiz, E. J.; Tolbert, S. H. *J. Phys. Chem. B* **2000**, *104*, 5448.
(6) Gross, A. F.; Le, V. H.; Kirsch, B. L.; Tolbert, S. H. *J. Am. Chem. Soc.* **2002**, *124*, 3713.
(7) Ågren, P.; Lindén, M.; Rosenholm, J. B.; Blanchard, J.; Schüth, F.; Amenitsch, H. *Langmuir* **2000**, *16*, 8809.
(8) Ågren, P.; Lindén, M.; Rosenholm, J. B.; Schwarzenbacher, R.; Kriechbaum, M.; Amenitsch, H.; Laggner, P.; Blanchard, J.; Schüth, F. *J. Phys. Chem. B* **1999**, *103*, 5943.
(9) Regev, O. *Langmuir* **1996**, *12*, 4940.
(10) O'Brien, S.; Francis, R. J.; Fogg, A.; O'Hare, D.; Okazaki, N.; Kuroda, K. *Chem. Mater.* **1999**, *11*, 1822.
(11) Lindén, M.; Ågren, P.; Karlsson, S.; Bussian, P.; Amenitsch, H. *Langmuir* **2000**, *16*, 5831.
(12) Lindén, M.; Schunk, S. A.; Schüth, F. *Angew. Chem., Int. Ed.* **1998**, *37*, 821.
(13) Lind, A.; Andersson, J.; Karlsson, S.; Ågren, P.; Bussian, P.; Amenitsch, H.; Lindén, M. *Langmuir* **2002**, *18*, 1380.
(14) Tiemann, M.; Goletto, V.; Blum, R.; Babonneau, F.; Amenitsch, H.; Lindén, M. *Langmuir* **2002**, *18*, 10053.
(15) Flodström, K.; Teixeira, C. V.; Amentisch, H.; Alfredsson, V.; Lindén, M. *Langmuir* **2004**, *20*, 4885.
(16) Flodström, K.; Wennerström, H.; Teixeira, C. V.; Amentisch, H.; Lindén, M.; Alfredsson, V. *Langmuir* **2004**, *20*, 10311.

Published on Web 05/24/2010

SBA-1 and SBA-3,[17,18] are synthesized in acidic medium. As a result, a complete different mechanism is assumed in which the cationic headgroup of the trialkylammonium surfactant and the positive charged silica species require a mediator ion for interaction. This is provided by the original halide counterion of the surfactant.

The synthesis of materials with pores up to 30 nm was first published in 1998.[19] The triblock copolymers consisting of ethylene oxide (EO) and propylene oxide (PO) units ($PEO_xPPO_yPEO_x$) opened up the possibility of varying the pore diameter in a relatively wide range. The hydrated PEO units form the hydrophilic shell (headgroups of the micelles) whereas the PPO units form the core (surfactant tails) of the micelles. The resulting formation mechanism of the mesophase is assumed to be a combination of hydrogen bonding, electrostatic, and van der Waals interactions. A prominent example following this mechanism is the SBA-15 silica.[20−22]

The appearance of a 3D hexagonal transition state during the formation of the 2D hexagonal mesophase has already been described in the literature. The 3D hexagonal structure was observed for the SBA-2 that is synthesized with gemini surfactants of the formula $C_{n-s-1}(C_nH_{2n+1}(CH_3)N-(CH_2)_s-N(CH_3)C_mH_{2m+1}$; in short, C_{n-s-m}).[23] The formation of the globular aggregate structure is ascribed to the large effective headgroup areas and the high charge density of the surfactants. In 1998, Zhao et al. described a phase transition from 3D hexagonal to 2D hexagonal caused by a hydrothermal treatment during the synthesis of the SBA-12 silica with Brij 76 as SDA.[20] The EO units of the nonionic surfactant Brij 76 appears to behave analogous to the large headgroups of the cationic surfactant species.[23−25] However, no data concerning the self-assembling process of 3D hexagonal ordered silica materials has been published up to now.

In 1999, a new class of porous materials, the so-called periodic mesoporous organosilica materials, was first introduced.[26−28] These materials show the same properties as the pure silica materials such as high ordering of the mesopores, high specific surface areas and narrow pore size distributions, despite they have organic units directly incorporated into the pore wall network. This can be achieved by applying an organosilica precursor of the formula $(OR)_3Si\text{-}R'\text{-}Si(OR)_3$ with R being methyl or ethyl and R′ being any organic unit. These materials offer new properties for applications like catalysis or separation.[29,30] Only few results have been published concerning their formation mechanism.[31] In situ SAXD investigations were described for a sample synthesized with octadecyltrimethylammonium chloride (OTAC) as structure-directing agent and 4,4′-bis(triethoxysilyl)-biphenyl (BTEBP) as organosilica precursor. This material showed a high ordering of units in the pore walls as well as a relatively high ordering of the mesopores (characterized by the occurrence of one diffraction peak in the low angle scattering region).[31]

For the synthesis of PMOs under acidic conditions, mostly Pluronic P123 or Brij-surfactants are used as SDAs.[32−41] In contrast to the synthesis in basic medium, the formation of the PMO materials under acidic conditions is quite fast. A white precipitation occurs within minutes after the addition of the organosilica precursor to the acidic solution of the SDA. This can be explained by the high velocity of hydrolysis and condensation reactions at pH values around zero. Thus, in situ SAXD is an excellent technique to study their self-assembling process. Here we report on the formation of 2D hexagonal ordered phenylene- and thiophene-bridged periodic mesoporous organosilicas synthesized with Brij 76 as SDAs in situ and ex situ.

Table 1. Molar Concentrations of the Investigated Samples

	BTEB	BTET	Brij 76	HCl	H_2O
sample 1[41]	0.5		0.2	0.52	287
sample 2		0.5	0.2	0.52	287

2. Experimental Section

Substances. Brij 76 and hydrochlocric acid were obtained from Aldrich. 1,4-bis(triethoxysilyl)benzene (BTEB) and 2,5-bis(triethoxysilyl)thiophene (BTET) were synthesized as described by Shea et al.[42] Table 1 gives the molar concentrations of the investigated samples.

(17) Kim, M. J.; Ryoo, R. *Chem. Mater.* **1999**, *11*, 487.
(18) Huo, Q.; Margolese, D. I.; Ciesla, U.; Feng, P.; Gier, T. E.; Sieger, P.; Leon, R.; Petroff, P. M.; Schüth, F.; Stucky, G. D. *Nature* **1994**, *368*, 317.
(19) Zhao, D.; Feng, J.; Huo, Q.; Melosh, N.; Fredrickson, G. H.; Chmelka, B. F.; Stucky, G. D. *Science* **1998**, *279*, 548.
(20) Zhao, D.; Huo, Q.; Feng, J.; Chmelka, B. F.; Stucky, G. D. *J. Am. Chem. Soc.* **1998**, *120*, 6024.
(21) Che, S.; Sakamoto, Y.; Terasaki, O.; Tatsumi, T. *Chem. Mater.* **2001**, *13*, 2237.
(22) Kruk, M.; Jaroniec, M. *Chem. Mater.* **2000**, *12*, 1961.
(23) Huo, Q.; Leon, R.; Petroff, P. M.; Stucky, G. D. *Science* **1995**, *268*, 1324.
(24) Israelachvili, J. N.; Mitchell, D. J.; Ninham, B. W. *J. Chem. Soc. Faraday Trans. 2* **1976**, *72*, 1525.
(25) Israelachvili, J. N.; Mitchell, D. J.; Ninham, B. W. *Biochim. Biophys. Acta* **1977**, *470*, 185.
(26) Inagaki, S.; Guan, S.; Fukushima, Y.; Ohsuna, T.; Terasaki, O. *J. Am. Chem. Soc.* **1999**, *121*, 9611.
(27) Yoshina-Ishii, C.; Asefa, T.; Coombs, N.; MacLachlan, M. J.; Ozin, G. A. *Chem. Commun.* **1999**, 2539.
(28) Melde, B. J.; Holland, B. T.; Blanford, C. F.; Stein, A. *Chem. Mater.* **1999**, *11*, 3302.
(29) Weitkamp, J.; Hunger, M.; Rymsa, U. *Microporous Mesoporous Mater.* **2001**, *48*, 255.
(30) Rebbin, V.; Schmidt, R.; Fröba, M. *Angew. Chem., Int. Ed.* **2006**, *45*, 5210.
(31) Morell, J.; Teixeira, C. V.; Cornelius, M.; Rebbin, V.; Tiemann, M.; Amentisch, H.; Fröba, M.; Lindén, M. *Chem. Mater.* **2004**, *16*, 5564.
(32) Morell, J.; Wolter, G.; Fröba, M. *Chem. Mater.* **2005**, *17*, 804.
(33) Muth, O.; Schellbach, C.; Fröba, M. *Chem. Commun.* **2001**, 2032.
(34) Burleigh, M. C.; Markowitz, M. A.; Wong, E. M.; Lin, J.-S.; Gaber, B. P. *Chem. Mater.* **2001**, *13*, 4411.
(35) Zhu, H.; Jones, D. J.; Zajac, J.; Rozière, J.; Dutartre, R. *Chem. Commun.* **2001**, 2568.
(36) Goto, Y.; Inagaki, S. *Chem. Commun.* **2002**, 2410.
(37) Matos, J. R.; Kruk, M.; Mercuri, L. P.; Jaroniec, M.; Asefa, T.; Coombs, N.; Ozin, G. A.; Kamiyama, T.; Terasaki, O. *Chem. Mater.* **2002**, *14*, 1903.
(38) Guo, W.; Park, J.-Y.; Oh, M.-O.; Jeong, H.-W.; Cho, W.-J.; Kim, I.; Ha, C.-S. *Chem. Mater.* **2003**, *15*, 2995.
(39) Bao, X. Y.; Zhao, X. S.; Li, X.; Chia, P, A.; Li, J. *J. Phys. Chem. B* **2004**, *108*, 4684.
(40) Cho, E.-B.; Char, K. *Chem. Mater.* **2004**, *16*, 270.
(41) Wang, W.; Zhou, W.; Sayari, A. *Chem. Mater.* **2003**, *15*, 4886.
(42) Shea, K. J.; Loy, D. A.; Webster, O. *J. Am. Chem. Soc.* **1992**, *114*, 6701.

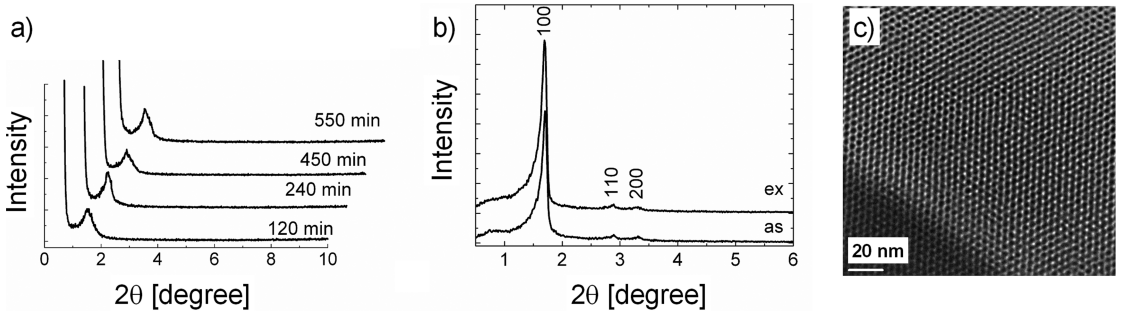

Figure 1. (a) Powder-XRD patterns of samples synthesized with different stirring times at a constant temperature of 50 °C. (b) Powder-XRD patterns of a sample synthesized with 120 min stirring time and a 24 h hydrothermal treatment at 105 °C (as, as-synthesized; ex, extracted). (c) TEM image of the extracted sample in b.

Measurements. In situ SAXD measurements were carried out at the soft condensed matter beamline A2 at DORIS III at HASYLAB/DESY, Hamburg, Germany. Data was taken using a monochromatic beam of wavelength 0.15 nm and a linear Gabriel type detector.

For the measurements a four neck reaction vessel with a reflux condenser was placed on a combined heater/stirrer and connected to a flow through capillary (inner diameter: 1.5 mm) by flexible tubing. The capillary was placed in the X-ray beam and the reaction solution was pumped through the setup with a flow of 26 mL/min during the experiment.[15,31]

Powder X-ray diffraction patterns were recorded with a Bruker AXS D8 Advance diffractometer at room temperature using filtered Cu−Kα radiation.

Sample preparation. Brij 76 was dissolved in 0.1 mol/L HCl and the reactions were started by the addition of the organosilica precursors BTEB and BTET, respectively. The reaction solutions were kept under continuous flow at 50 °C which were interrupted when the resulting solid particles in the solution were about to block the capillary. All investigations were repeated three times in order to prove the reproducibility of the experiment. After finishing the measurements, the products were filtered off and washed with water, dried in air, and solvent-extracted in a Soxhlet apparatus for 6 h with a mixture of ethanol/HCl (100:3; v:v).

In addition, samples were also synthesized in the laboratory by stirring the same reaction solution mixture up to 24 h. Some samples were subsequently hydrothermally treated at 105 °C for 24 h. All products were washed with water and dried in air. Removal of the surfactant was done by solvent extraction in a Soxhlet apparatus for 6 h with a mixture of ethanol/HCl (100:3; v:v).

3. Results

3.1. Phenylene-Bridged PMOs. Brij 76 consists of an octadecyl chain and 10 ethylene oxide (EO) units. The EO units are a little more hydrophilic than the alkyl chain and form the headgroup of the surfactant. We assume the chain of EO units to be in coiled configuration. The octadecyl chain is the hydrophobic part and therefore the "tail" of the surfactant.

The powder X-ray diffraction (P-XRD) patterns of the samples synthesized in the laboratory with different stirring times but without subsequent hydrothermal treatment are depicted in Figure 1a. XRD patterns of the sample stirred for 2 h and treated at 105 °C are shown in Figure 1b (as, as-synthesized, ex, extracted), the TEM image of the extracted sample is given in Figure 1c.

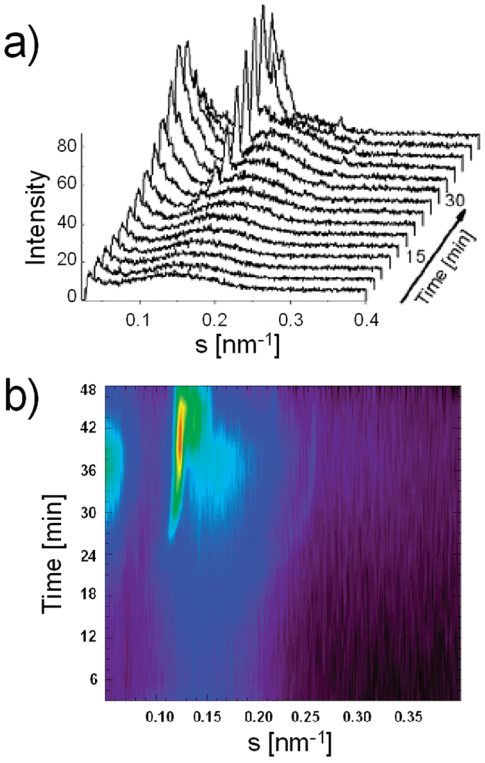

Figure 2. (a) Evolution of the SAXD patterns of the sample containing Brij 76 as SDA and BTED as organosilica precursor measured at 50 °C. (b) Contour plot of the evolution of the SAXD patterns of the sample in part a.

One can see that the additional hydrothermal treatment at 105 °C leads to a highly 2D hexagonal ordered material (d_{100} = 5.23 nm, d_{110} = 3.05 nm, d_{200} = 2.64 nm). All samples synthesized without a hydrothermal treatment show only one reflection in the XRD pattern with a repeat distance of 5.5 nm. The contraction of the mesostructure is induced by ongoing condensation at high temperatures (105 °C) caused by the hydrothermal treatment.

The synthesis procedure of the sample containing BTEB as organosilica precursor was investigated by small-angle X-ray diffraction. The evolution of the SAXD pattern taken at a constant temperature of the solution of 50 °C and a pH of 1 is depicted in Figure 2a. For better illustration, a contour plot is shown in Figure 2b.

One can deduce that the fast hydrolysis and condensation at pH 1 lead to precipitation almost immediately with

the addition of the organosilica precursor. Higher temperatures increase the reaction velocity, which makes the hydrothermal treatment temperature at 105 °C impossible to follow by time-resolved SAXD because of the fast increase in the particle size and thus, the short time period of continuous flow of the suspension.

The first seven measurements show only a broad profile as patterns, which can be ascribed to diffuse scattering of particles. After 21 min of reaction time, a structure showing one sharp diffraction peak with a corresponding repeat distance of 9.47 nm evolved. Only three minutes later a second reflection (d = 4.21 nm) appeared in the pattern. With proceeding time, the lattice parameter of the structure decreased, evidenced by a parallel shift of both diffraction peaks to higher s values. An ordering increase is concluded by the higher intensity and the sharper profile of the reflections. The intensity of the broad profile increases until three additional reflections occur after 39 min. Finally, after 42 min reaction five diffraction peaks can be clearly identified: d_1 = 7.98 nm, d_2 = 7.25 nm, d_3 = 6.77 nm, d_4 = 4.61 nm, d_5 = 3.89 nm.

3.2. Thiophene-Bridged PMOs. Similar measurements were carried out using 2,5-bis(triethoxsilyl)thiophene (BTET) instead of 1,4-bis(triethoxysilyl)benzene (BTEB) as organosilica source. The molar concentrations were the same as for the sample containing BTEB (see Experimental Section, Table 1). The powder samples without and with hydrothermal treatment lead to the same results, as shown above for the phenylene-bridged samples. Samples synthesized without hydrothermal treatment show only one reflection but the samples with additional hydrothermal treatment produced a well-defined 2D hexagonal mesostructure (not shown here). The evolution of the SAXD patterns with time is given in Figure 3a. The corresponding repeat distances deduced from the diffraction peaks are depicted in Figure 3c.

Note that this sample allowed to monitor the reaction up to 96 min therefore more data could be taken and, compared to the sample synthesized with BTEB as organosilica precursor, showing that under these synthesis conditions the resulting structures at the end are stable and no further change in the lattice parameters could be detected.

The evolution of the structure is nearly the same as previously described for the samples synthesized with BTEB. Figure 3b shows a broad scattering profile from the beginning of the data acquisition due to diffuse scattering of particles in the solution (○).

A structure, first showing one diffraction peak (●, d = 5.8 nm), evolves after 5 min reaction time and a second reflection can be detected after 30 min (■, d = 10.8 nm). From the beginning of the structural evolution (5 min) a contraction of the structure can be observed reaching a constant lattice parameter after 60 min reaction time. During the contraction of the structure the diffuse scattering (right-pointing triangle) oscillates again when three further reflections arise (▲, ▼, ◆) after 70 min.

For both systems studied, the evolution of the structure was found to be nearly the same, independent of the

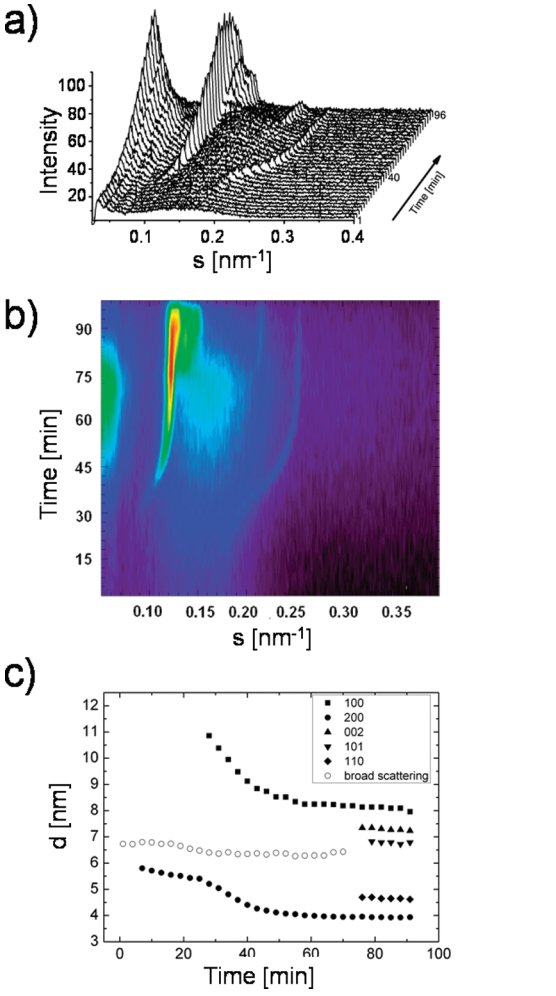

Figure 3. (a) Waterfall diagram and (b) contour plot of the synthesis evolution for the sample containing Brij 76 as SDA and BTET as organosilica source. The reaction was monitored at a constant temperature of 50 °C. (c) Evolution of the repeat distances for the diffraction peaks identified from the measurement of the sample containing BTET as organosilica source (Figure 3c).

organic unit of the organosilica precursor. The values for the repeat distances are very similar, which can be expected because of the similar size of the organic units. However, an indexing to clearly identify one single phase is not possible in both cases.

For both samples, a broad profile ascribed to diffuse scattering is observed directly after the addition of the organosilica precursor. From the occurrence of the first mesostrucure diffraction peak a slight difference between the two samples could be observed: For the sample synthesized with BTET, the evolution of the structure starts with the occurrence of the (200) reflection of the 2D hexagonal mesostructure followed by the (100) reflection after 30 min reaction time, whereas the sample synthesized with BTEB shows first the (100) and then the (200) reflection some minutes later. For both samples, the intensity of the broad profile increases with contraction of the mesostructure. With the occurrence of additional three diffraction peaks, the broad profile and thus the scattering continuously decrease until it vanishes. For both samples, these three diffraction peaks can

Table 2. Repeat Distances and Lattice Parameters of the Single Reflections Indexed for the 2D and 3D Hexagonal Mesostructures

	BTEB ($p6mm$)	BTEB ($P6_3/mmc$)	BTET ($p6mm$)	BTET ($P6_3/mmc$)
d_{100} (nm)	7.98	7.98	7.95	7.95
d_{002} (nm)		7.25		7.23
d_{101} (nm)		6.77		6.78
d_{110} (nm)	4.61	4.61	4.60	4.60
d_{200} (nm)	3.98		3.93	
a^a (nm)	9.21	9.21	9.17	9.17
c^a (nm)		14.50		14.46
c/a		1.58		1.58

[a]

$$a = \frac{2}{3}\sqrt{3}d_{100}$$

where c can be calculated from ref 43:

$$\sin^2\theta = \frac{\lambda^2}{4a^2}\left[\frac{4}{3}(h^2+k^2+hk)+\left(\frac{a}{c}\right)^2 l^2\right]$$

with h, k, l being the Miller indices, a and c being the unit-cell parameters of the 3D hexagonal mesostructure, and λ being the wavelength of the synchrotron beam (0.15 nm).

be indexed to the (002), (101), and (110) reflections of the 3D hexagonal mesophase (hexagonal close packed spheres, hcps, space group: $P6_3/mmc$), whereas the (110) reflection fits also to the 2D hexagonal structure (hexagonal close-packed cylinders, hcpc, space group $p6mm$).

The results of the SAXD measurements for both samples are summarized in Table 2.

4. Discussion

The syntheses of the 2D hexagonal structured materials carried out in the laboratory let us expect a 2D hexagonal mesostructure during the in situ investigations. Three of the five occurring reflections fit well to the 2D hexagonal structure ((100), (110), (200)). The two additional diffraction peaks can be indexed to the (002) and (101) of the 3D hexagonal phase (space group: $P6_3/mmc$). Thus, in both cases a coexistence of a 2D and a 3D hexagonal mesophase was found. The lattice constants a (for the 2D hexagonal phase) and a and c (for the 3D hexagonal phase) are also given in Table 2. For the 3D hexagonal structure, we obtain a ratio c/a of 1.58, which is in good agreement with the ideal c/a ratio of 1.633. These calculations corroborate the coexistence of the 2D and 3D hexagonal structures. An isolation of the material during the structure forming process with both structures was not possible.

Comparing our results to the synthesis of SBA-12, several parallels could be drawn. Even before the organosilica precursor was added to the solution, a broad scattering profile could already be observed. This shows that the concentration of the surfactant is above the critical micelle concentration and thus, aggregation of subunits to large particles are the reason for the diffuse scattering.

With the addition of the organosilica precursors to the solutions the diffuse scattering increases while the micelles start to form particles of disordered aggregates. Different research groups have shown that these so-called particles are separated droplets of disordered micelles,[44−46] but such properties cannot be uniquely shown by X-ray diffraction. The formation process is driven by the polymerizing organosilica species because the surfactant concentration in the solution is too low to form a liquid crystal. The ordering takes place by the varying number of charges on the surface of the silica species during hydrolysis and condensation. The broad scattering decreases with the ongoing ordering process. The occurrence of the (100) and (200) reflections of the 2D hexagonal phase as well as the broad scattering profile show that disordered particles, ordered spherical, and ordered cylindrical micelles coexist in the solution. After about 30 min reaction time, the cylindrical micelles and the spherical micelles become organized and the (100), (110), and (200) reflections are evidence for highly ordered close-packed cylindrical micelles in the solution, whereas the (100), (002), (101), and (110) reflections show the appearance of highly ordered hexagonal close-packed spheres.

A comparison between the described samples − laboratory synthesis without hydrothermal treatment (Figure 1a), laboratory synthesis with hydrothermal treatment (Figure 1b), and the in situ synthesis (Figure 2a) − show that all samples were investigated at different stages of the reaction. The powder sample synthesized without hydrothermal treatment, which was filtered off after 120 min and dried in air, shows only one reflection with a repeat distance of 5.5 nm. We assume a poor ordered structure that can be two- or three-dimensional or even both. Regarding the results described by Zhao et al.[20] for the synthesis of the SBA-12 the three-dimensional structure is more probable. However, a clear indexing of the structure is impossible with these data.

The in situ reaction leads to a structure showing the first diffraction peak with a repeat distance of 7.98 nm after about 42 min reaction time. Compared to the heat-treated powder sample (Figure 1b) showing a 2D hexagonal structure with d_{100} = 5.2 nm, we can conclude that the reaction is at a very early stage; even after 120 min, the degree of hydrolysis and condensation is still low. During the in situ experiment, we measure the composite material which includes all surfactant and organosilica in the complex solution system. At early stages of the reaction, the partly hydrolyzed and condensed silica species are connected to the headgroup of the surfactant molecules by electrostatic and van der Waals interactions. An interruption of the reaction at this stage followed by washing with water leads to a partial destruction of the composite due to the low degree of condensation. This can be seen for the powder samples in Figure 1a, which

(43) Massa, W. *Kristallstrukturbestimmung 2*; Teubner: Stuttgart, Germany, 1996.

(44) Chan, H. B.; Budd, P. M.; Naylor, T. deV. *J. Mater. Chem.* **2001**, *11*, 951.

(45) Brennan, T.; Roser, S. J.; Mann, S.; Edler, K. J. *Chem. Mater.* **2002**, *14*, 4292.

(46) Flodström, K.; Wennerström, H.; Alfredsson, V. *Langmuir* **2004**, *20*, 680.

show only a poor ordered structure. Nevertheless, the hydrolysis and condensation is ongoing during the drying process and leads to a contraction of the structure and thus to a decrease in its size.

The complete vanishing of the 3D hexagonal phase after heating the reaction solution to 105 °C shows that this is a metastable transition state. We assume the spherical micelles to elongate to cylinders during the heating step. This can be explained by the changing polarity of the EO units at higher temperatures. At lower temperatures, the headgroup consisting of 10 EO units is relatively large. From this fact we expect curved micelles like spheres or cylinders. As shown in the plots (Figure 2b, Figure 3b), we observe coexisting cylindrical and spherical micelles after the addition of the organosilica precursor. Normally we would expect an increase in the micelle curvature with ongoing condensation because of charge density matching. But we have to take into account that the EO units and their conformation are quite sensitive to the reaction temperature. At low temperatures, the EO units′ conformation is anti-gauche-anti (a-g-a), which exhibits a higher polarity as anti-anti-anti (a-a-a) which is the dominating conformation at high temperatures. Thus, the hydrothermal treatment leads to a decrease in the headgroup area of the surfactant by changes in the EO units′ conformations.[47] A decrease of the headgroup size a_0 leads to an increase in the ion pair packing parameter g and thus to a lower curved surface and results in the 2D hexagonal phase after the hydrothermal treatment of the solution.

(47) B. Jönnson, Lindmann, B.; Holmberg, K.; Kronberg, B., *Surfactants and Polymers in Aqueous Solutions*; John Wiley & Sons: New York, 1998.

5. Conclusions

From these experiments, we can conclude that the two different organosilica precursors BTEB and BTET react in the same way under these synthesis conditions. Even the lattice parameters of the resulting structures are nearly the same. The more interesting result was the evolution of the structures during the experiments. A coexistence of two different phases at a very early stage of the reaction was found but it could be shown that after a hydrothermal treatment only the 2D hexagonal structure was left in the material. An isolation of the 3D hexagonal phase was in both cases not possible, which is evidence that this structure is an intermediate state. This let us compare our data with that of the SBA-12 pure silica material. Although no in situ data of the formation of the SBA-12 silica exist, clear similarities in the resulting structures after the room temperature synthesis and the synthesis containing a hydrothermal treatment can be shown. A synthesis at room temperature led to a 3D hexagonal ordered material and an additional hydrothermal treatment caused a phase transition to a 2D hexagonal structure. Our in situ experiments show similar results. The in situ investigations at 50 °C lead to the formation of a 3D and a 2D hexagonal structure, a hydrothermal treatment completes the phase transition from 3D to 2D hexagonal. From these results, we can conclude that under these synthesis conditions, the influence of the organic unit of the BTEB compared to the pure silica precursor is low.

Acknowledgment. The authors thank Martin Dommach (Hasylab) for technical support at beamline A2. For the TEM image, Günter Koch (JLU Giessen) is gratefully acknowledged.